Bacteria Modified Stainless Steel Anode for Glucose Fuel Cell

Y. Tahiri[1*], S. Zahid[1], M. Oubaouz[1], M. Oukbab[1], H. Haddouchy[3], A. Zaroual[2], S. E. El Qouatli[3] and A. Chtaini[1]

[1]*Electrochemistry and Molecular Inorganic Materials Team, Faculty of Sciences and Technology, Sultan Moulay Slimane University, Beni Mellal, Morocco*
[2] *Department of Chemistry and Environment, Faculty of Science, Mohammed V University, Rabat, Morocco*
[3]*Laboratory of Physical Chemistry Environment and Material, Moulay Ismail University, Faculty of Sciences and Technologies, Errachidia, Morocco*
*Corresponding author: youness.tahiri@usms.ma

Received 10/06/2024; accepted 30/11/2024
https://doi.org/10.4152/pea.2026440505

Abstract
Electrooxidation (EO) of glucose (Glu) on a stainless steel (SS) electrode surface was investigated under two conditions: in the absence and presence of *Pseudomonas* bacteria. In its absence, CV analysis revealed a redox system within potential (E) range from -0.5 to 0 V. However, when bacteria suspension was introduced into the electrolytic solution, significant changes were observed. CV showed the emergence of anodic and cathodic peaks, accompanied by a substantial increase in current density (j). This indicated strong interactions between electrode surface and bacteria. The presence of bacteria also caused the redox system to shift towards more anodic E values. Despite this shift, oxidation j decreased. These findings suggest that *Pseudomonas* played a critical role in modifying the electrochemical behavior of Glu on SS electrode surface, possibly through direct interactions or alterations in the local environment at the electrode-electrolyte interface.

Keywords: bio-corrosion; CV; EO; Glu; *pseudomonas*; SS.

Introduction•

The increasing reliance on fossil fuels requires the exploration of alternative energy sources. One promising solution is the conversion of biomass into fundamental chemicals [1-6]. Biomass is abundant in nature, motivating researchers to develop suitable conversion methods. Glu, a derivative of biomass, can be used to generate electrical energy through fuel cells [7, 8]. Glu-based fuel cells, which operate via its complete oxidation, can release substantial energy up to 3 mJ/mol [9]. Glu offers several advantages as a fuel, including its wide availability, low cost and non-toxicity [10-13]. Moreover, Glu eliminates explosion risks and storage challenges commonly associated with hydrogen and methanol, both of which are highly flammable. Thus, Glu fuel cells are emerging as promising alternatives [14-16].

•The abbreviations and symbols definition lists are in page 390.

In parallel, significant advancements in medical implants have shifted focus from passive to active implants, incorporating electronic devices that can monitor and regulate bodily functions. These active implants may include sensors or energy sources, such as Li-I_2 battery used in pacemakers [17, 18].
In healthcare, Glu fuel cells are particularly advantageous, due to their ability to achieve significant volumetric reduction. Instead of storing energy, they directly convert Glu, a fuel readily available in the body, into electrical energy. This feature, combined with their ease of implantation, allows Glu fuel cells to function and generate energy from virtually any location within the body. For instance, polymer-electrolyte Glu fuel cells can employ various bodily fluids, such as interstitial fluid or blood, as a fuel source for energy generation, tears or cerebrospinal fluid [19-21]. Glu complete oxidation requires the use of living micro-organisms, such as bacteria, which can generate energy up to 1000 $\mu W/cm^2$ [22].
In this paper, the performance of a SS electrode for Glu oxidation in presence of bacteria was examined.

Experimental

The experiments were carried out in an electrochemical measuring cell equipped with Ag-AgCl, Pt (1 cm^2) and SS (1 cm^2) plates, as reference, auxiliary/counter and working electrodes, respectively. A potentiostat type Volta lab 10 was assisted by Master 4 software. The electrolyte used was a 1 M NaCl solution.
Dark-field optical microscope, with a specialized condenser, provided high resolution (0.2 μm), 10x–100x magnification, contrast enhancement for unstained specimens, and image capture, enabling clear visualization and analysis of bacterial adhesion.
Powdered Glu was from Sigma-Aldrich, with a purity of ≥ 99.5% and mass of 180.16 g/mol. Bacteria used in this work were *Pseudomonas* (Gram-negative). The strain was cultivated in *Luria Bertani* broth, at 37°C, for 24 h. Cells were then harvested by centrifugation at 8400 xg, for 15 min, washed twice, and resuspended in a 0.1 M KNO_3 solution. Physicochemical properties were assessed using contact angle measurements. Oxygen was removed by bubbling N gas through the solution, for 5 min, and maintaining a N blanket during the experiment. A fresh solution was prepared for each experiment. The bacterial suspension was diluted with water to the required concentration. For *Pseudomonas* cultured in *Luria Bertani* broth, at 37°C, for 24 h, optical density at 600 nm typically ranged from 0.8 to 1.5, depending on growth conditions.

Results and discussion

Interaction of bacteria with the SS surface

Fig. 1 (a-b) shows the images taken by optical microscope for SS plates without and with bacteria (in a solution, for 15 min), respectively. The choice of 15 min immersion time for the electrode in the solution with *Pseudomonas* was because it allowed optimal adhesion of the bacteria to the electrode surface, while

maintaining their biological viability. This time was experimentally optimized to ensure good electrochemical performance, and it is easily reproducible, thus guaranteeing reliable and consistent results in experiments. Fig. 1 shows adhesion of bacterial spherical structures onto the SS surface.

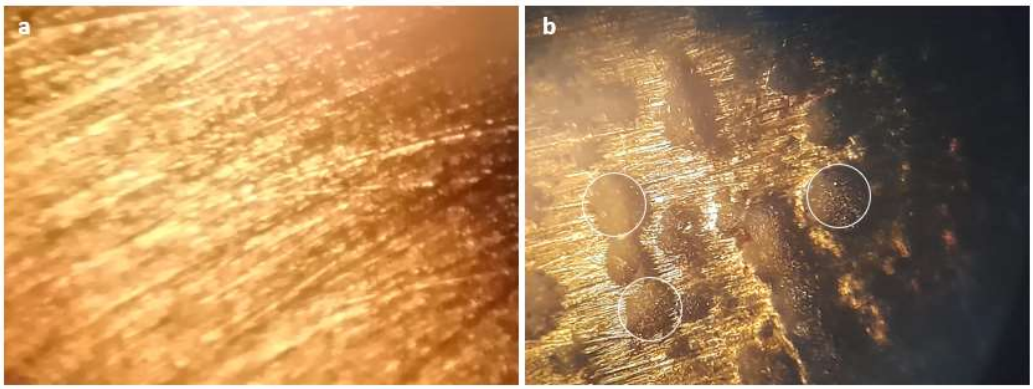

Figure 1: Optical microscope images of SS surface- **(a)** without bacteria; **(b)** with bacteria, after 15 min.

Mechanism of bacterial action on Glu oxidation

Aerobic bacteria employ a process known as cellular respiration, to oxidize Glu and harness energy in the form of adenosine triphosphate [23-25]. This cellular respiration occurs in several stages: glycolysis, Krebs cycle (also referred to as citric acid cycle) and electron transport chain. Overall reaction for aerobic respiration can be summarized as follows:

$$\text{Glucose} + \text{O} \longrightarrow \text{CO}_2 + \text{H}_2\text{O} + \text{Energy (in ATP form)}$$

Another pathway involves Glu oxidation to gluconate, at the membrane level, facilitated by the enzyme gluconate dehydrogenase, as illustrated in Fig. 2.

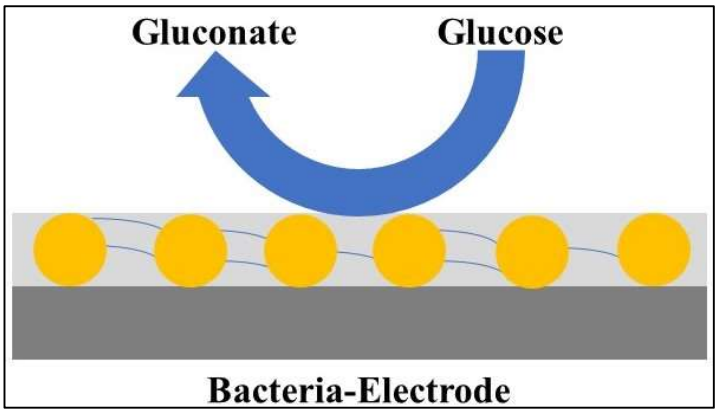

Figure 2: Image showing glucose oxidation to gluconate.

Fig. 3 shows CV recorded on the SS electrode surface, in 1 M NaCl solutions without (curve a) and with bacteria (curve b).

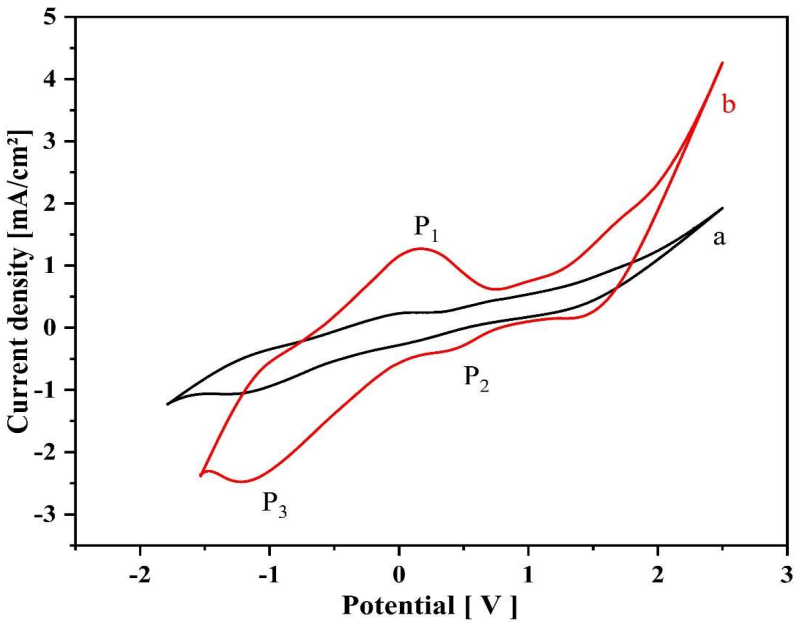

Figure 3: CV recorded at the SS electrode in a 1 M NaCl solution - **(a)** without and **(b)** with bacteria.

Pseudomona presence in the electrolyte medium caused a remarkable change in the CV structure, since they have redox properties. The CV shows a well-defined peak (P_1), in anodic scanning direction, around 0.1 V, and two reduction peaks, in cathodic scanning direction, P_2 and P_3, at 0.5 and around -1 V, respectively.
Fig. 4 shows the effect of bacteria contact with the electrode surface. As the contact time increased, j of redox peaks increased, shifting towards positive (P_1) and negative E (P_2 and P_3), respectively.

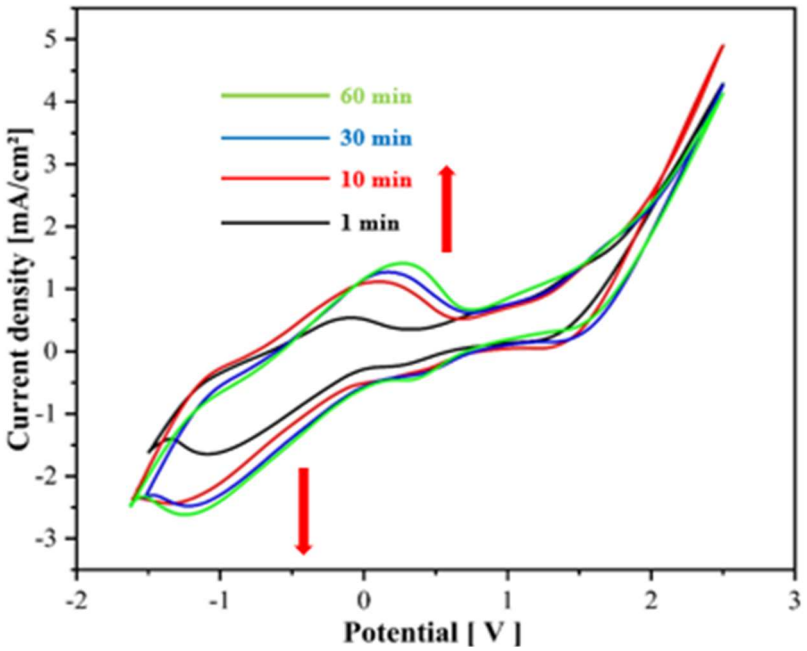

Figure 4: CV recorded at the SS electrode, in 1 M NaCl with *Pseudomonas*, and effect of pre-concentration time.

The shift in redox peaks towards more positive and negative E values, respectively, suggests a modification in the electrochemical environment at the electrode-bacteria interface. Several possible interpretations for this include: change in microenvironment-the bacteria, by forming a biofilm or releasing substances, can alter the microenvironment near the electrode, which lead to a change in redox conditions (E, local pH, etc.); variation in electroactive mediators- the shift in peaks may be associated with the release or consumption of redox mediators by bacteria, or with a modification in the dynamics of electron transfer reactions; and reduction of electron transfer barrier- the formation of a bacterial biofilm could lower the energy barrier for electron transfer, resulting in a change in reaction E.
Table 1 gathers electrochemical parameters deduced from impedance diagrams. C_{dl} evolution, which increased considerably with contact time of bacteria with the electrode surface, is seen, confirming their adhesion onto it.

Table 1: Electrochemical parameters.

Time [min]	Diameter [KΩ.cm^2]	Correlation	R_1 [Ω.cm^2]	R_2 [Ω.cm^2]	$R_2 - R_1$ [Ω.cm^2]	C_{dl} [µf/cm^2]
0	0.140	0.980	28.29	139	110.71	57.22
1	1.082	0.990	320.4	1077	756.6	165.3
5	0.912	0.999	268	911.4	643.4	174.6
10	0.850	0.987	266.3	843.0	576.7	264.2
15	0.760	0.989	246.7	755.8	509.1	294.8
90	0.592	0.983	192.9	590.8	397.9	339.4

The effect of scan rate (SR) on CV curve recorded at the SS electrode surface in the bacteria presence is depicted in Fig. 5.

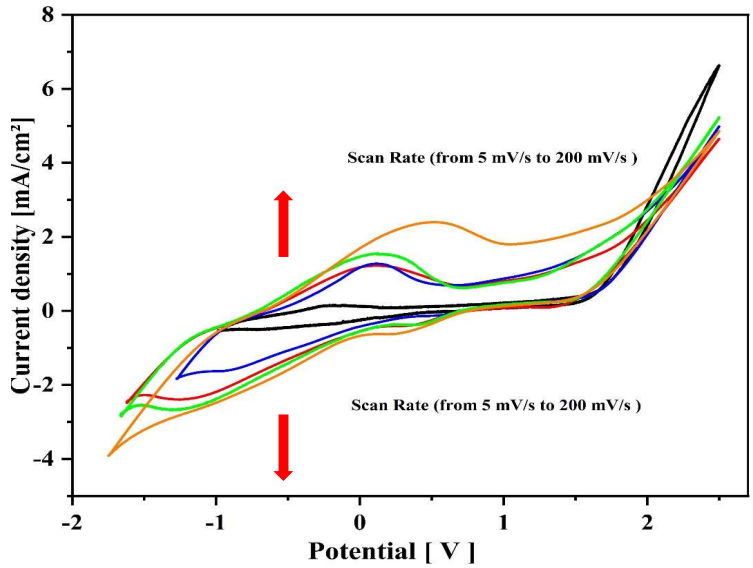

Figure 5: CV recorded at SS electrode, in 1 M NaCl with bacteria. SR effect.

By analysing these results, a linear increase in peak j with higher SR is observes. This indicates that, within this range of SR values, the system proportionally

responded to SR variations, which suggests a diffusion-controlled electrochemical behaviour. In other words, at moderate SR, electron transport is fast enough for surface reactions to closely follow changes in SR.
However, when SR became very high, this linear relationship weakened, since, at these values, the increase in peak j occurred much more slowly. This shift in trend can be attributed to the quasi-reversible nature of the system (depicted in Fig. 6).

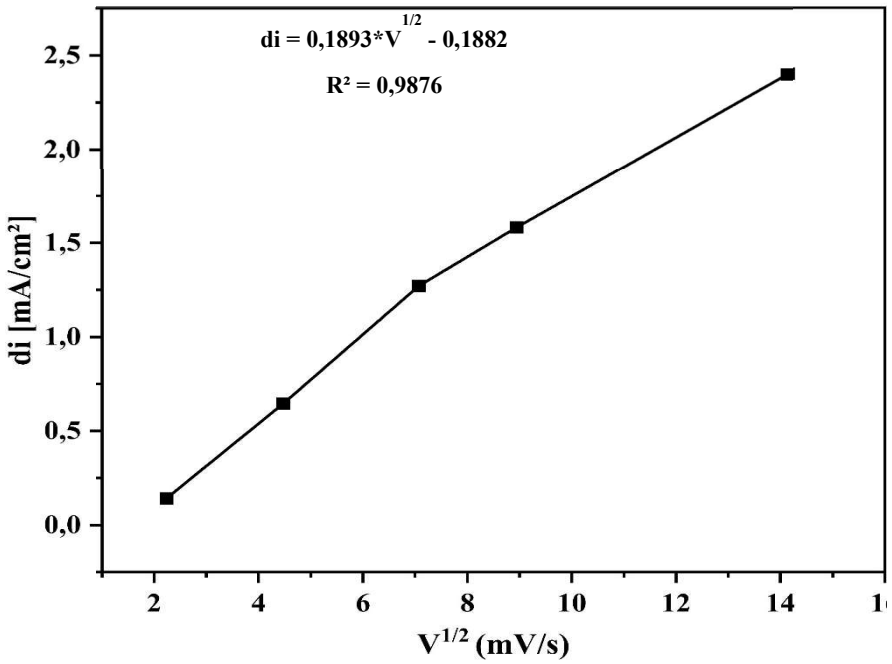

Figure 6: Evolution of anodic peak j with SR square root.

In electrochemical terms, a quasi-reversible system is characterized by a less pronounced balance between the surface reaction rate and charge transport (electrons and ions). In this case, the electron transfer processes start to lag behind rapid changes in SR, resulting in a relative decrease in peak j.
This transition to a quasi-reversible regime at high SR suggests kinetic limitations in electron transfer processes between SS electrode and bacteria. The nature of these limitations could be related to factors such as charge transfer barriers at the electrode-bacteria interface, modifications in biofilm layer structure, or even saturation of reactive sites on the electrode surface. These results highlight the importance of electrode-bacteria interactions in overall electrochemical response, providing a deeper understanding of the mechanisms involved in biologically-coupled metallic electrode systems.

EO of Glu on the surface of the SS electrode

The oxidation of Glu on the SS electrode surface, in a 1 M NaCl solution, was studied by CV. Glu oxidation on the of the SS electrode surface, in a 1 M NaCl, was studied by CV.
Fig. 7 shows CV recorded without (curve a) and with (curve b) Glu.

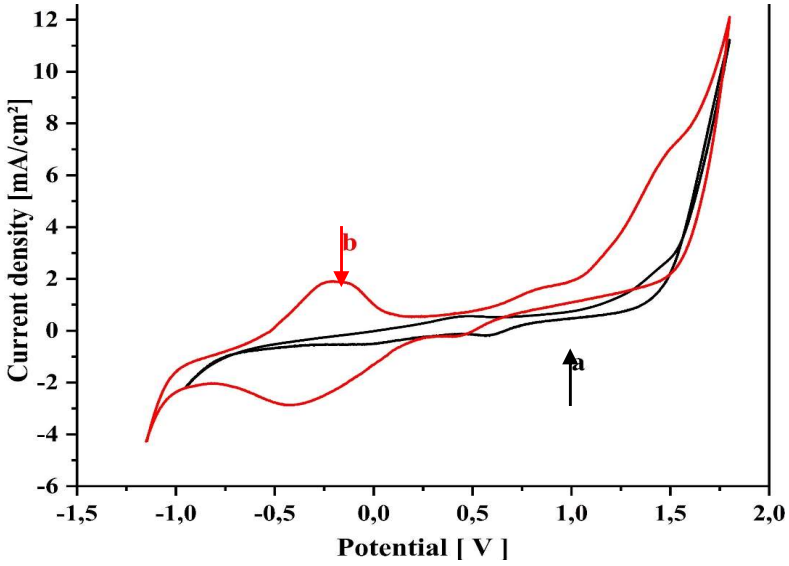

Figure 7: CV recorded at the SS electrode in 1 M NaCl - (**a**) without (**b**) and with glucose.

Glu oxidation is characterized by two opposite peaks: the first is anodic, at approximately -0.25 V, while the second is cathodic, at about -0.5 V, indicating a redox system. Notably, anodic j values were significantly higher.
Fig. 8 presents SWV results obtained at the SS electrode surface, both without (curve a) and with (curve b) Glu. Glu oxidation is evident from the appearance of three peaks in SWV. The first peak was around -0.5 V, the second at -0.25 V, corresponding to Glu initial redox reaction, and the third, at around 1.5 V, represents an oxidation peak.

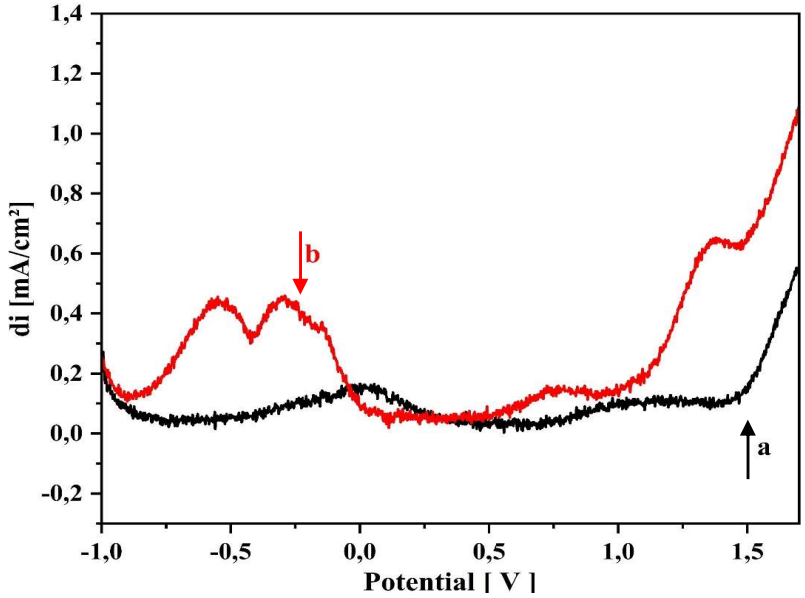

Figure 8: SWV recorded at SS electrode in 1 M NaCl - (**a**) without (**b**) and with glucose.

Fig. 9 shows EIS diagrams recorded on the SS electrode surface without (curve a) and with Glu (curve b). EIS diagrams have the shape of half-loops, of which

diameter corresponds to R_{ct}. R_{ct} value was smaller in Glu presence than in its absence, which shows the electrode activity towards Glu oxidation.

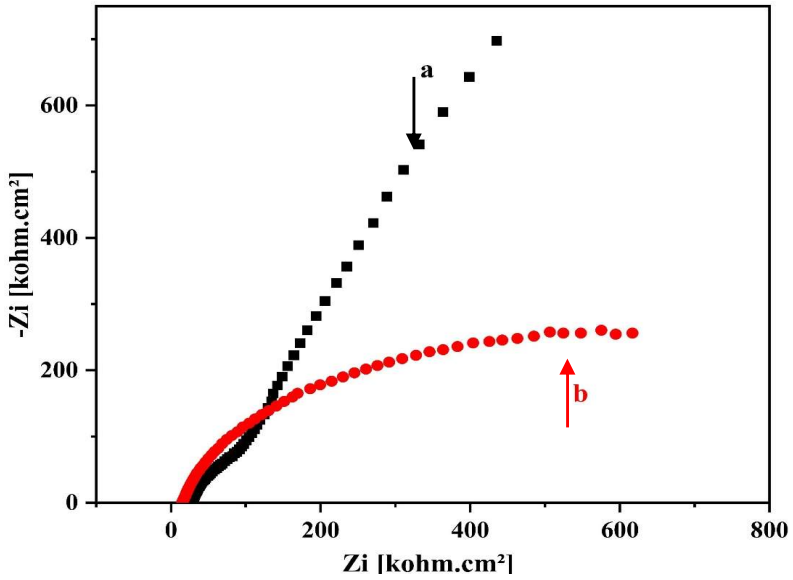

Figure 9: EIS recorded at SS electrode in 1 M NaCl - (**a)** without (**b)** and with glucose.

The oxidation reaction can be considered as an electron transfer, which was studied by plotting Taffel lines (Fig. 10). Curve (a) was recorded in NaCl without Glu and curve (b) with it. It was seen that Glu presence shifted equilibrium E towards negative values, which shows the activity of this electrode towards Glu oxidation.

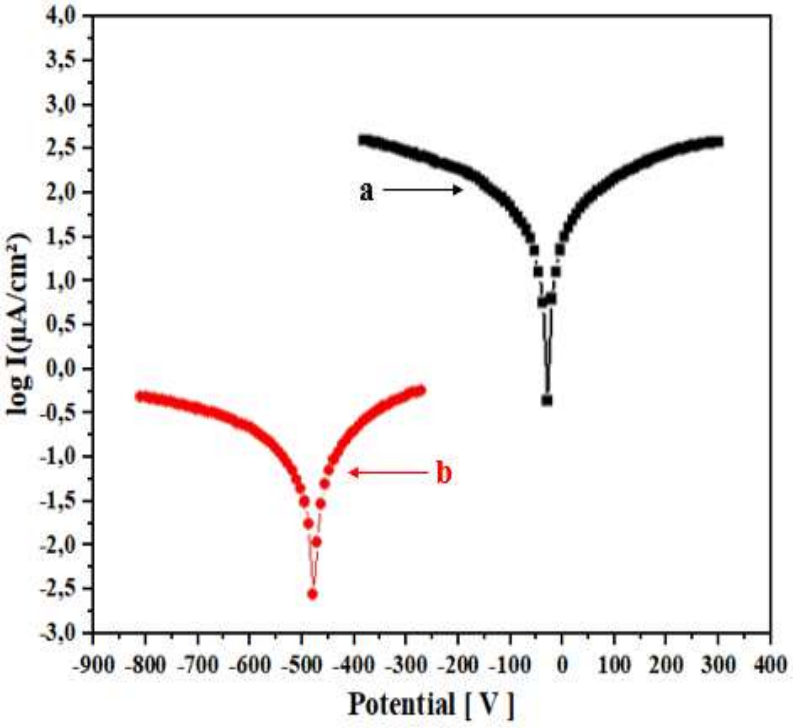

Figure 10: Taffel plots recorded at the SS electrode in 1 M NaCl- (**a**) without and (**b)** with glucose.

Table 2 summarizes electrochemical parameters deduced from Tafel curves. As it is seen, equilibrium E went from -35.5 V, in Glu absence, to -480.9 V, in its presence. Therefore, Glu oxidation was favored. The j value recorded at equilibrium went, in Glu absence, from 233.9 to 0.652 mA/cm^2, in its presence, which means that it has formed a film on the electrode surface. The anodic slope increased, in Glu absence, from 1113.3 to 589.1 mV, in its presence, which shows that the reaction was controlled by oxidation.

Table 2: Electrochemical parameters.

Electrode	E(i=0) (mV)	R_p (Ω.cm^2)	i_{corr} (mA/cm^2)	β_a (mV)	β_c (mV)	Coefficient	CR (mm/Y)
SS	-35.5	676.5	233.9	1113.3	1067.8	1	2.7
SS-Glu	-480.9	160.7	0.6	589.1	1079.1	1	7.6

Electro oxidation of Glu on the SS electrode surface in bacteria presence

Glu oxidation with bacteria was studied on the SS electrode surface. Fig. 11 shows CV recorded at the SS electrode surface in NaCl with Glu and *Pseudomonas*.

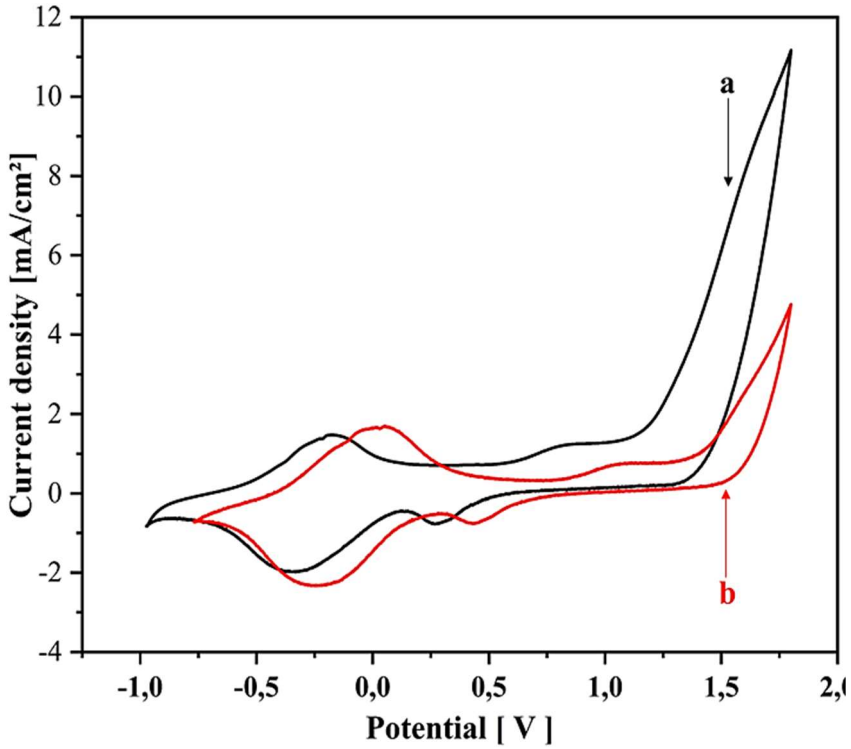

Figure 11: CV's recorded at the SS electrode in 1 M NaCl- **(a)** with *Pseudomonas* and (**b**) with bacteria and glucose.

CV, in Glu absence (curve a) and presence (b), had the same shape. Redox peaks appeared at shifted E values. However, j decreased for Glu oxidation in bacteria presence.

SWV recorded on the SS electrode surface in NaCl with bacteria (curve a) and Glu (curve b), are presented in Fig. 12. It was found that j increased in Glu presence.

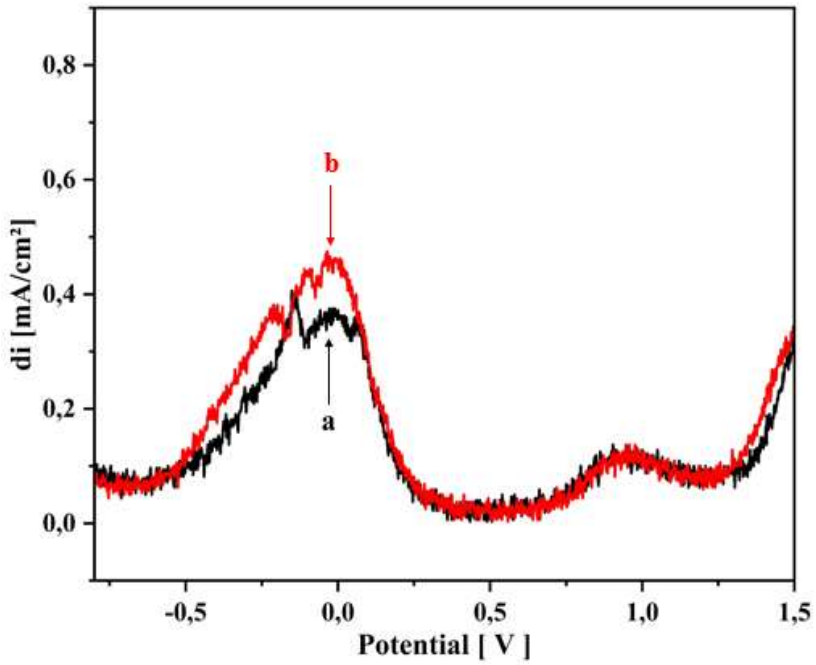

Figure 12: SWV recorded at the SS electrode in 1 M NaCl- **(a)** with bacteria and (**b**) with bacteria and glucose.

Fig. 13 shows EIS recorded on the SS electrode surface in NaCl with bacteria, without (curve a) and with Glu (curve b). EIS have the shape of half-loops, of which diameter corresponds to electron R_{ct}. Glu oxidation manifested by a decrease in R_{ct}, which corresponds to an increase in the electrode activity.

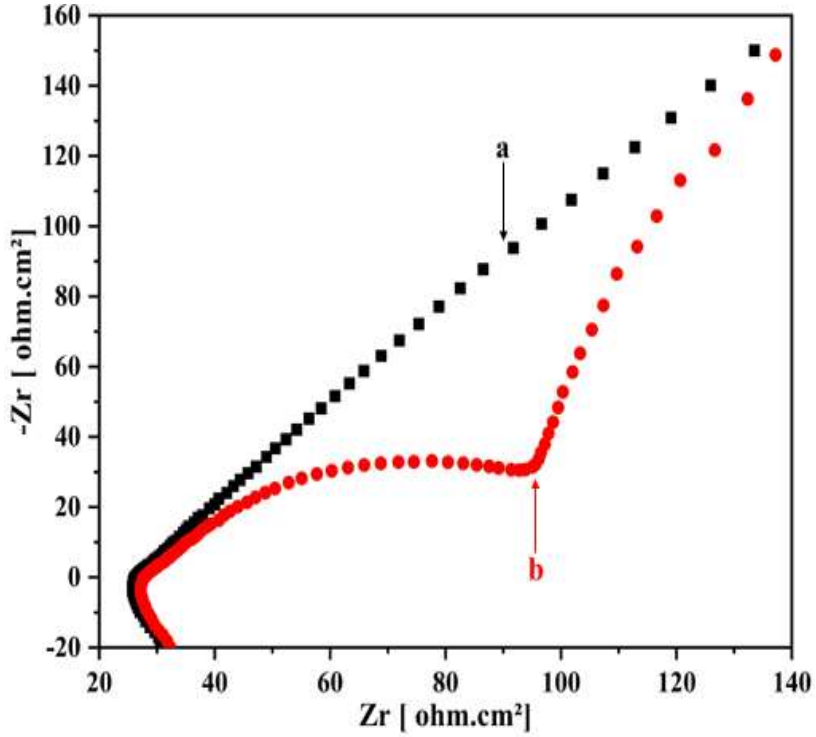

Figure 13: EIS recorded at the SS electrode in 1 M NaCl- **(a)** with bacteria and (**b**) with bacteria and glucose.

The j of peaks relating to Glu oxidation in the presence of bacteria linearly varied with Glu concentration (Fig. 14), for which an analytical equation was determined.

$E = -0{,}0182*[C_6H_{12}O_6] - 0{,}1995$
$R^2 = 0{,}9957$ Peack P_1

$E = -0{,}0182*[C_6H_{12}O_6] - 0{,}1995$
$R^2 = 0{,}9957$ Peack P_2

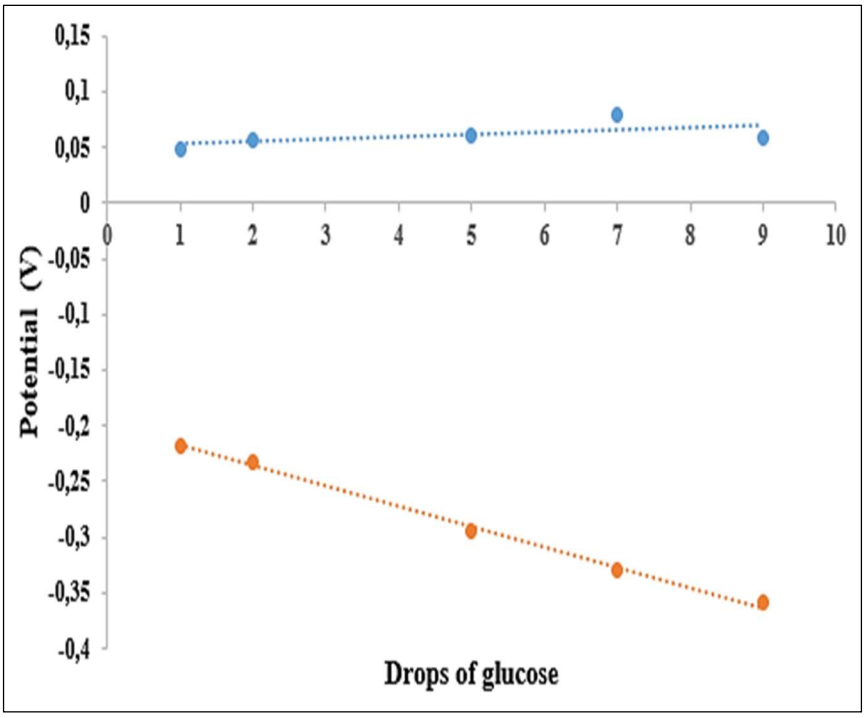

Figure 14: Evolution of anodic and cathodic peaks j with Ct of glucose in 1 M NaCl with bacteria.

Conclusions

In conclusion, Glu fuel cells present a promising solution for a variety of applications in medical electronic implants, particularly as power sources for heart stimulators and as biosensors. SS electrode utilized in these fuel cells has demonstrated impressive performance in terms of Glu oxidation efficiency, achieving significant j, while showing no signs of surface poisoning.

Furthermore, the innovative incorporation of *Pseudomonas* as catalysts for Glu oxidation offers a compelling advancement in this field. These bacteria tend to modify the electrode surface by forming a biocompatible biofilm, which not only enhances catalytic activity, but also promotes integration with biological tissues. Notably, the bioelectrode retained the same functional properties as the bare electrode surface, ensuring reliable performance in real world applications. This dual capability underscores the potential of Glu fuel cells to improve the safety and efficacy of medical devices, paving the way for more sustainable and efficient power sources in healthcare technology.

Acknowledgements
We acknowledge the Molecular Electrochemistry and Inorganic Materials Team Faculty of Science and Technics, Beni Mellal, Morocco.

Authors' contributions
Y. Tahiri: corresponding author; did experimental protocol; reviewed and edited original draft of the manuscript; made modifications asked by referees and editor. **S. Zahid**, **M. Oubaouz**, **M. Oukbab**, **H. Haddouchy**, **A. Zaroual and S. E. El Qouatli**: contributed to project supervision, experimental investigation and conceptualization. **A. Chtaini**: acted as supervising professor; elaborated experimental protocol; wrote initial draft of manuscript.

Abbreviations
β_a: anodic Tafel slope
β_a: cathodic Tafel slope
C_{dl}: double layer capacity
CV: cyclic voltammetry/voltammogram
E: potential
EIS: electrochemical impedance spectroscopy
EO: electrochemical oxidation
Glu: glucose
i_{corr}: corrosion current density
j: current density
NaCl: sodium chloride
R_{ct}: charge transfer resistance
redox: reduction/oxidation reaction
R_p: polarization resistance
SR: scan rate
SS: stainless steel
SWV: square wave voltammetry/voltammogram

References
1. Besson M, Gallezot P, Pinel C. Conversion of biomass into chemicals over metal catalysts. Chem Rev. 2014;114:1827-1870. https://doi.org/10.1021/cr4002269
2. Mika LT, Cséfalvay E, Németh Á. Catalytic conversion of carbohydrates to initial platform chemicals: chemistry and sustainability. Chem Rev. 2017;118:505-613. https://doi.org/10.1021/acs.chemrev.7b00395
3. Liu C, Wang H, Karim AM et al. Catalytic fast pyrolysis of lignocellulosic biomass. Chem Soc Rev. 2014;43:7594-7623. https://doi.org/10.1039/C3CS60414D
4. Zakzeski J, Bruijnincx PCA, Jongerius AL et al. The catalytic valorization of lignin for the production of renewable chemicals. Chem Rev. 2010;110:3552-3599. https://doi.org/10.1021/cr900354u

5. Huber GW, Iborra S, Corma A et al. Synthesis of transportation fuels from biomass: chemistry, catalysts, and engineering. Chem Rev. 2006;106:4044-4098. https://doi.org/10.1021/cr068360d
6. Bozell JJ. Connecting biomass and petroleum processing with a chemical bridge. Science. 2010;329:522-523. https://doi.org/10.1126/science.1191662
7. Zhang Z, Huber GW. Catalytic oxidation of carbohydrates into organic acids and furan chemicals. Chem Soc Rev. 2018;47:1351-1390. https://doi.org/10.1039/C7CS00213K
8. Van Putten R-J. Hydroxymethylfurfural, a versatile platform chemical made from renewable resources. Chem Rev. 2013;113:1499-1597. https://doi.org/10.1021/cr300182k
9. Antolini E. External abiotic glucose fuel cells. Sust Ener Fuels. 2021;5:5038-5060. https://doi.org/10.1039/D1SE00727K
10. Dai YX, Ding J, Li JY et al. N, S and Transition-Metal Co-Doped Graphene Nanocomposites as High-Performance Catalyst for Glucose Oxidation in a Direct Glucose Alkaline Fuel Cell. Nanomaterials. 2021;11:202. https://doi.org/10.3390/nano11010202
11. Dong F, Liu XH, Irfan M et al. Macaroon-like $FeCo_2O_4$ modified activated carbon anode for enhancing power generation in direct glucose fuel cell. Int J Hydrog Ener. 2019;44:8178-8187. https://doi.org/10.1016/j.ijhydene.2019.02.031
12. Gao MY, Liu XH, Irfan M et al. Nickle-cobalt composite catalyst-modified activated carbon anode for direct glucose alkaline fuel cell. Int J Hydrog Ener. 2018;43:1805-1815. https://doi.org/10.1016/j.jpowsour.2013.11.013
13. Hao MQ, Liu XH, Feng MN et al. Generating power from cellulose in an alkaline fuel cell enhanced by methyl viologen as an electron-transfer catalyst. J Pow Sour. 2014;251:222-228. https://doi.org/10.1016/j.jpowsour.2013.11.013
14. Ho J, Li Y, Dai YX et al. Ionothermal synthesis of N-doped carbon supported $CoMn_2O_4$ nanoparticles as ORR catalyst in direct glucose alkaline fuel cell. Int J Hydrog Ener. 2021;46:20503-20515. https://doi.org/10.1016/j.ijhydene.2021.03.145
15. Irfan M, Khan IU, Wang et al. 3D porous nanostructured Ni_3N-Co_3N as a robust electrode material for glucose fuel cell. RSC Adv. 2020;10:6444-6451. https://doi.org/10.1039/C9RA08812A
16. Rismani-Yazdi H, Christy AD, Dehority BA et al. Electricity generation from cellulose by rumen microorganisms in microbial fuel cells. Biotechnol Bioeng. 2007;97:1398-1407. https://doi.org/10.1002/bit.21366
17. Sanders RS. In: Cardiac Pacing for the Clinician. Eds: Kusumoto FM, Goldschlager NF, Springer US, Boston, MA, USA. 2008:47-71. https://doi.org/10.1007/978-0-387-72763-9
18. Greatbatch W, Lee WJ, Mathias W et al. IEEE Trans. A New Method for Measuring the Dynamic Properties of Biological Tissues. Biomed Eng. 1971;18:317. https://doi.org/10.1002/advs.202307369

19. Kerzenmacher S, Ducrée J, Zengerle R et al. Energy harvesting by implantable abiotically catalyzed glucose fuel cells. Pow Sour. 2008;182(1):1-17. https://doi.org/10.1016/j.jpowsour.2008.03.031
20. Reid RC, Minteer SD, Gale BK. Electrochemical biosensors for the detection of small molecules: a review. Biosens Bioelectron. 2015;68:142. https://doi.org/10.1016/j.bios.2014.12.034
21. Rapoport BI, Kedzierski JT, Sarpeshkar R. A Computational Model of the Hippocampus: Representing the Integration of Sensory and Cognitive Information. PLoS One. 2012;7: e38436. https://doi.org/10.1371/journal.pone.0038436
22. Bullen RA, Arnot TC, Lakeman JB et al. Biofuel cells and their development. Biosens Bioelectron. 2006;21:2015-2045. https://doi.org/10.1016/j.bios.2006.01.030
23. Alberts B, Johnson A, Lewis J et al. Molecular Biology of the Cell. 4th edition. New York: Garland Science; 2002. ISSN (online): 1939-4586
24. Latour X, Lemanceau P. Métabolisme carboné et énergétique des Pseudomonas spp fluorescents saprophytes à oxydase positive. Agronomie. 1997;(17)9-10:427-443. https://doi.org/10.1051/AGRO:19970901
25. Tremblay YD, Hathroubi S, Jacques M et al. Les biofilms bactériens: leur importance en santé animale et en santé publique. Canad J Vet Res. 2014;(78)2:110-116. PMCID: PMC3962273; PMID: 24688172.